Transport in Porous Media of Highly Concentrated Iron Micro- and Nanoparticles in the Presence of Xanthan Gum

ARTICLE *in* ENVIRONMENTAL SCIENCE AND TECHNOLOGY · DECEMBER 2009

Impact Factor: 5.33 · DOI: 10.1021/es901897d · Source: PubMed

3 AUTHORS, INCLUDING:

Michela Luna
Politecnico di Torino
3 PUBLICATIONS **85** CITATIONS
SEE PROFILE

Rajandrea Sethi
Politecnico di Torino
67 PUBLICATIONS **1,185** CITATIONS
SEE PROFILE

Transport in Porous Media of Highly Concentrated Iron Micro- and Nanoparticles in the Presence of Xanthan Gum

ELENA DALLA VECCHIA, MICHELA LUNA, AND RAJANDREA SETHI*

DITAG - Dipartimento di Ingegneria del Territorio, dell'Ambiente e delle Geotecnologie, Politecnico di Torino, Corso Duca degli Abruzzi, 24 10129, Torino, Italy

Received June 27, 2009. Revised manuscript received October 5, 2009. Accepted October 16, 2009.

The ability of xanthan gum to act as a delivery vehicle for the transport in porous media of highly concentrated nano- and microscale zerovalent iron (NZVI and MZVI, respectively) slurries was investigated. Sand-packed column experiments were performed injecting iron suspensions at a concentration of 20 g/L, amended with xanthan gum (3 g/L), at different ionic strength values (6×10^{-3} mM or 12.5 mM) in 0.46 m long columns. Breakthrough curves of iron, obtained by in-line continuous measurement of magnetic susceptibility, under each experimental condition showed that normalized elution concentration at the end of the injection (i.e., after 7 or 26 pore volumes) is higher for MZVI (>0.94) than for NZVI (>0.88). Additional susceptibility measurements along the column and pressure drop also confirmed that MZVI is more easily eluted than NZVI. Moreover, water flushing after the iron injection phase lead to recoveries of over 95% for MZVI, and over 92% for NZVI of the total injected iron mass. The tests proved that xanthan gum is an excellent stabilizing agent and delivery vehicle of ZVI particles and has a high potential for use in real scale remediation interventions.

Introduction

The reactivity of zerovalent iron (ZVI) toward a wide array of contaminants, which includes both organic and inorganic compounds, renders the use of this material one of the most versatile groundwater remediation approaches (*1, 2*). Granular ZVI fillings have been successfully employed in permeable reactive barriers (PRBs) (*3, 4*). However, in recent years, the attention of environmental engineers and scientists has been driven toward micro- or nanoscale ZVI (MZVI or NZVI, respectively). Thanks to their high specific surface area, these materials exhibit a much higher reactivity toward the contaminants. Additionally, MZVI and NZVI have the potential to be suspended in aqueous slurries and injected in the subsurface in the direct vicinity of the target, the delivery of the particles to the contaminated plume downgradient being enhanced by the groundwater flow.

One of the major limitations of both MZVI and NZVI water dispersions is their high colloidal unstability, hence their use for remediation interventions is hindered by the uncertainties concerning their successful delivery to the source of contamination. MZVI, being in the size range of most favorable transport in natural groundwater (*5*), is nevertheless affected by the tendency to sediment under the effect of gravity. NZVI is subject to strong attractive interparticle forces which overcome repulsive ones, leading to particle aggregation (*6–8*). Formation of NZVI aggregates, widely exceeding the nanoscale, will on the one hand decrease reactivity, and on the other hand promote plugging of the porous media, thus impeding further mobility of the particles due to straining and gravitational settling. Aggregation is therefore highly undesirable (*9–12*). Furthermore, iron nanoparticle shells are constituted of iron oxides which are likely to have a strong affinity for adsorption onto surfaces of soil grains (*11*). This will also negatively affect the transportability of nanoiron through porous media (*13*). In order to optimize the delivery of the reactive particles to the target of contamination and maximize the radius of influence achievable during the injection phase, it is essential to successfully stabilize the iron slurries. A strategy typically adopted to enhance suspension stability is surface modification with surfactants or block-co-polymers (e.g., polyacrilic acid, starch, amphiphilic triblock copolymers, carboxymethylcellulose, guar gum, polyaspartate). By coating the particles, these amendments are able to provide steric, electrostatic, or electrosteric stabilization (*12, 14, 15*). This has been shown to offer the means for effective iron particle transport. However, the success of these delivery vehicles was only proven for low particle loadings, up to a maximum of 6 g/L (*8–12, 15–20*).

The goals of this present study are (1) to assess the transportability of highly concentrated MZVI and NZVI suspensions amended with xanthan gum as a delivery vehicle with respect to bare particle suspensions; (2) to investigate whether long-term injection phases lead to clogging phenomena and hinder particle transport; and (3) to investigate the effect of increased ionic strength (IS) on the elutability of the suspension.

We hereby present a series of column experiments, comparing the transport under different conditions of highly concentrated (20 g/L) suspensions of MZVI and NZVI particles, either bare or modified with xanthan gum. Xanthan gum was selected as a suitable material for its high potential as a delivery vehicle, based on its stabilizing capability and for its rheological characteristics. Solutions of this polymer have a shear thinning behavior that can be explained in terms of progressive destruction of intermolecular low-energy bonds established through polysaccharide chains (*21*). As reported by Comba and Sethi (*21*) suspensions made of 3 g/L of xanthan are characterized by a viscosity of 1.1 Pa·s, at shear rates of 0.5 s^{-1}, that decreases to 1.1×10^{-2} Pa·s when the shear rate increases to 500 s^{-1}. These rheological properties are retained also after, and are hardly affected by, the dispersion of ZVI micro- or nanoparticles (*21–24*). This suggests that during injection, the delivery of dispersed particles in porous media may be possible thanks to the viscosity decrease of the suspension under high shear rates reached during injection.

In this work we employ an original method to measure the concentration of the elute which exploits the ferromagnetic nature of iron. By measuring the magnetic susceptibility of the slurry at the outflow we were able to derive the concentration of the elute in time. This strategy proved extremely valuable since it provided a continuous logging of the breakthrough curve also using highly concentrated dispersions.

* Corresponding author email address: rajandrea.sethi@polito.it.

10.1021/es901897d CCC: $40.75
Published on Web 10/30/2009

Experimental Section

Materials. *MZVI Particles.* Experiments were conducted with micro and nanoscale iron dispersions, either bare or treated with a surface modifier. Micrometric particles (BASF-HQ) were purchased from BASF (Germany) and stored as a powder. Their nominal size ranges from 1 to 3 μm and they are composed of 98.4% Fe and of 1.6% carbon, nitrogen, and oxygen impurities.

NZVI Particles. Commercial reactive iron nanoparticles (RNIP-10DS) were supplied by Toda Kogyo Corp. (Onoda, Japan). These particles are characterized by an average size of 70 nm prior to aggregation. They are composed of a core of elemental iron, representing approximately 65% of each particle, coated by a shell of iron oxides, mainly magnetite (Fe_3O_4). RNIP-10DS is provided and was stored as a dispersion in deionized (DI) water at a concentration of approximately 30% wt.

Xanthan Gum. A high molecular weight (5×10^6 g/mol) polymer, xanthan gum (Jungbunzlauer, Switzerland), was used as a stabilizing agent for the ZVI suspensions. Ultrapure DI water, with an IS of approximately 6×10^{-3} mM, was employed in all experiments as a dispersing medium. $CaCl_2$ and NaCl (Sigma-Aldrich) were used to adjust the salt concentration for the high IS experiments.

Silica Sand. Silica sand, with the following grain size distribution: $d_{10} = 0.46$ mm, $d_{50} = 0.69$ mm, $d_{90} = 1.03$ mm, was provided by Sibelco (Robilante, Italy) and used as model porous medium for column experiments. Prior to use, the sand was subjected to sequential cleaning steps as described in Tiraferri and Sethi (*12*).

Methods. *ZVI Dispersions Preparation.* ZVI dispersions with a particle concentration of 20 g/L were prepared immediately prior to each experiment. First, the RNIP-10DS slurry or the BASF-HQ powder were diluted in water, either deionized or with 8 mM NaCl and 1.5 mM $CaCl_2$ to obtain a final IS of 12.5 mM. Particles were disaggregated by stirring the dispersions with a centrifugal mixer for 10 min while immersed in a sonication bath. Surface modification was attained by adding previously prepared xanthan gum solution (22 g/L) to achieve a final polymer concentration of 3 g/L. The concentration of 3 g/L was chosen because it prevents the settling of both the MZVI and NZVI for more than 5 h. Therefore it provides enough stability to the suspensions to avoid any loss of material in the pumping system and in the column during the tests. The same concentration would be suitable for fields operation where it would be possible to prepare the suspensions on-site.

Transport Experiments. MZVI and NZVI transport experiments were performed through sand packed, 0.46 m long Plexiglas columns with 2.4 cm internal diameter. Polypropylene caps were used to connect the column to 0.8 cm outer diameter Rilsan tubing. A sand prefilter, 1 cm thick and with 1−2 mm grain size, was introduced at both ends of the column. The column was packed to a porosity of 0.49, measured gravimetrically. Hydraulic conductivity, $K = 5.7 \times 10^{-3}$ m/s (permeability, $k = 5.81 \times 10^{-10}$ m^2), was determined using a constant-headwater permeameter. One pore volume (PV) equals 1.0×10^{-4} m^3. During slurry injection, the column was positioned horizontally to simulate more realistic flow conditions. The dispersions and flushing solutions were injected into the column by using a Masterflex L/S EASY-LOAD2 laboratory peristaltic pump. An inflowing discharge $Q = 6.7 \times 10^{-7}$ m^3/s was used. All the suspensions were kept unstirred during injection phase. An apparent viscosity of 5×10^{-2} Pa·s of the suspensions during the permeation through the column was calculated by applying Darcy's law (*25*) to the pressure drop registered in the initial phase of the injection (600 mbar). According to the experimental data reported by Comba and Sethi (*21*) this viscosity corresponds to a shear rate of 90 s^{-1}.

Four different transport conditions were investigated for both NZVI and MZVI. In three of the experiments the injection phase lasted 7 PV, with the iron particles being suspended either in DI water, in 3 g/L xanthan gum with an IS of 6×10^{-3} mM, or in xanthan gum with an IS of 12.5 mM. For simplicity, in the rest of this paper these experiments will be called N7W, N7X, N7X_IS, respectively, where NZVI is used, and M7W, M7X, M7X_IS, respectively, where MZVI is used. In the fourth experiment, the iron slurry (i.e., particles dispersed in 3 g/L xanthan gum, IS = 6×10^{-3} mM) was injected for 26 PV, in order to investigate pore clogging after a long injection phase. This experiment will be called N26X or M26X, in the case of NZVI or MZVI slurries, respectively. Prior to the start of the actual experiment, the column was preconditioned with 4 PV of solution having the same IS value of the ZVI slurry to be injected and circum-neutral pH. At the end of the injection phase, 15 PV of the same solution were used to perform a first flushing of the column, followed by a second flushing with 10 PV of DI water.

Magnetic Susceptibility-Based Breakthrough Curve Measurements. A MS2 magnetic susceptibility sensor (Bartington Instruments, UK) was positioned at the outflow of the column allowing for continuous measurement of the susceptibility value of the elute. The sensor consists of an AC wound inductor which determines the frequency of an oscillator based on the magnetic permeability (and thus susceptibility) of the sample and has a nominal resolution of 2×10^{-6} SI units.

According to Bregar and Pavlin (*26*), for a dispersion of ferromagnetic particles the relationship between concentration and susceptibility is linear. Given this relation, by exploiting the magnetic properties of iron it was possible to build a single point calibration algorithm to convert susceptibility to concentration values (data not reported).

Iron Distribution along the Column. At the end of the injection phase of the experiments M7X_IS and M7X_IS the susceptibility sensor allowed a non destructive measurement of the distribution of the magnetic material, i.e., iron particles, along the length of the column. The measurement was performed at 21 points along the column, under zero flow conditions, before starting the flushing phase. Calibration of the instrument was carried out by using calibration cylinders provided by the producer as well as prepared specifically for this purpose. An algorithm was developed for the spatial decorrelation of the signal in order to retrieve the iron concentration in correspondence of the sensor (not reported).

Pressure Drop Measurement. As a complement to the acquisition of the breakthrough curve, the pressure drop between the two ends of the column was measured in continuous during the whole length of the experiments. A PCE-P50 (PCE Group, Italy) differential manometer was used.

Results and Discussion

Transport of MZVI and NZVI through Porous Media. Iron breakthrough curves and the corresponding pressure drop curves between the two ends of the column over time are plotted in figures 1a-f. The breakthrough curves of the unmodified particle suspensions are not shown because of the very low yield they provided. However, percentages of eluted material in these experiments are reported in Table 1. Scarce mobility of unmodified iron particles has been reported by previous studies and was expected (*9*−*11*, *17*, *27*). It is mainly attributable to the instability of unsupported iron dispersions, which leads to particle aggregation, in the case of NZVI, and to gravitational settling (*6*). Additionally, attractive interaction forces between the grains of the solid matrix and the suspended particles, both nano- and microscale, may contribute to filtration phenomena (*5*, *15*, *28*).

Breakthrough curves of iron in the presence of xanthan gum under each experimental condition show that microscale

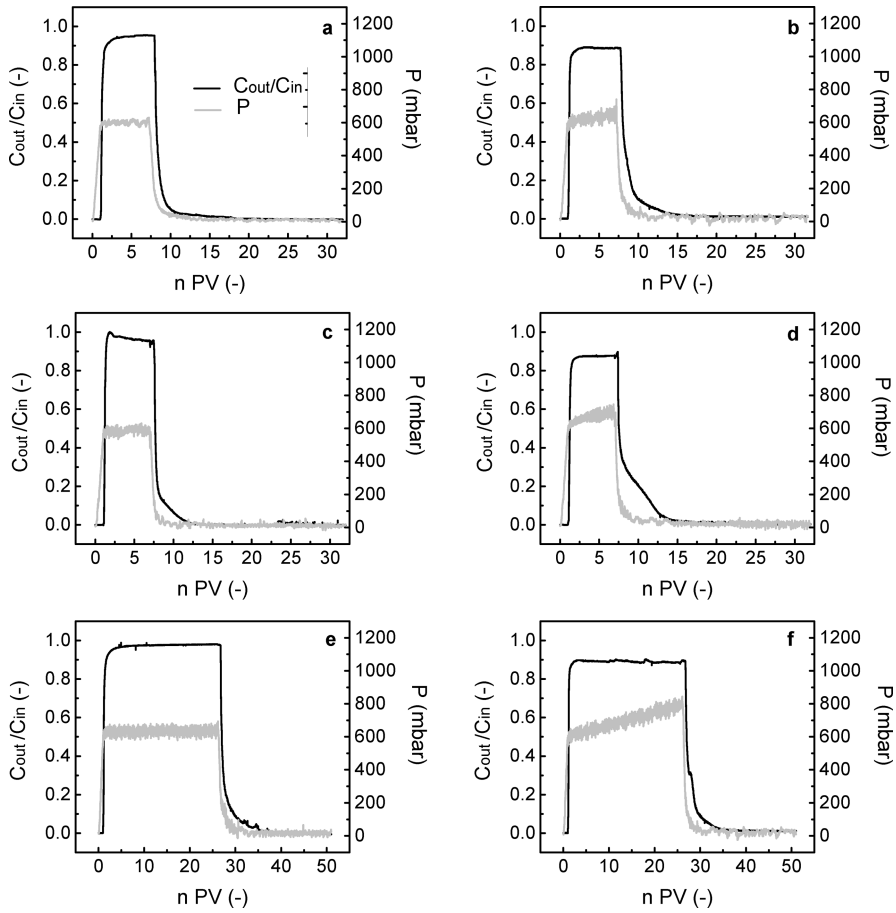

FIGURE 1. Breakthrough curves (solid black line) and corresponding pressure drop between the two ends of the columns (solid gray line). In each row curves are compared for the same transport conditions for MZVI (left column) and NZVI (right column). (a) M7X and (b) N7X: injection phase lasting 7 PV, IS of the suspension equal to 6 × 10^{-3} mM; (c) M7X_IS and (d) N7X_IS: injection phase lasting 7 PV, IS of the suspension equal to 12.5 mM; (e) M26X and (f) N26X: injection phase lasting 26 PV, IS of the suspension equal to 6 × 10^{-3} mM.

TABLE 1. Summary of Susceptibility, Concentration and Pressure Drop Measurements during the Column Experiments[a]

	M7W	M7X	M7X_IS	M26X	N7W	N7X	N7X_IS	N26X
t_{in}(s)	1050	1050	1050	3900	1050	1050	1050	3900
C_{max}/C_{in}	<0.01	0.95	0.94	0.97	<0.01	0.88	0.88	0.89
η' (−)	0%	77%	80%	93%	21%	73%	72%	85%
η (−)	1%	99%	95%	99%	22%	99%	96%	92%
M_r(g)	14.1	3.2	2.9	3.9	11.1	3.8	4.0	7.9
P_{max}(mbar)	–	608	581	630	–	646	696	789

[a] *Experiments Description, M*) experiment conducted with MZVI; *N*) experiment conducted with NZVI; 7W) ZVI suspended in DI water, injection phase lasting 7 PV, IS value of the suspension equal to 6 × 10^{-3} mM; 7*X*) ZVI suspended in 3 g/L xanthan gum, injection phase lasting 7 PV, IS value of the suspension equal to 6 × 10^{-3} mM; 7X_IS) ZVI suspended in 3 g/L xanthan gum, injection phase lasting 7 PV, IS value of the suspension equal to 12.5 mM; 26*X*) ZVI suspended in 3 g/L xanthan gum, injection phase lasting 26 PV, IS value of the suspension equal to 6 × 10^{-3} mM. *Measured Parameters*, t_{in}) iron slurries injection time; η') iron yield at the end of the injection phase; η) iron yield at the end of the test; *M*) residual mass of iron inside the column; P_{max}) maximal pressure drop between the two ends of the column at the end of the injection time.)

particles always reach a higher elution concentration at the end of the injection than nanoscale particles. The maximum values attained by the ratio between eluted and injected iron concentration (C_{max}/C_{in}) in the case of MZVI are 0.95, 0.94, and 0.97 in the M7X, M7X_IS, and M26IS experiments, respectively, against the 0.89, 0.88, and 0.89 values in the case of NZVI, in the corresponding experiments (Table 1). This suggests that during the transport through the porous medium a higher percentage of iron nanoparticles may accumulate within the column.

Evolution of the Pressure Drop between the Ends of the Column during ZVI Transport. Figure 1a−f also show how the pressure drop between the two ends of the column changes during the experiment (values to be read on the second *y*-axis). Regardless of the particle type, a steep increase in the value of pressure is evident when the injected liquid is switched from water to the iron slurry. This is consistent with the increase in viscosity of the eluting fluid.

By comparing the evolution of the pressure drop with time in the different experiments a remarkable difference can be depicted between the MZVI and the NZVI in correspondence of the concentration plateau in the breakthrough curves. In the experiments conducted with microscale iron dispersions, also the pressure drop reaches a

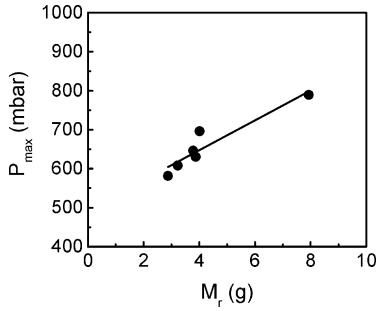

FIGURE 2. Linear relation between the mass of iron retained within the porous medium at the end of the injection phase (M_r) and the maximal pressure drop (P_{max}) between the inlet and the outlet of the column. Full circles (●) are the experimental measurements of mass and pressure for each experiment, the solid line (—) is the linear regression with an R^2 of 0.85 (intercept: 494.5 mbar, slope: 38.2 mbar/g).

maximum and maintains this value for the whole of the slurry injection phase. In contrast, in the nanoscale iron dispersion experiments, the pressure drop continuously grows even once the concentration of the elute reaches its maximum. Because the injected fluid and its flow rate are constant during this phase, it is reasonable to attribute the increasing pressure to a partial occlusion of the pores in the solid matrix, which is in agreement with the hypothesis of accumulation suggested by the nonunitary values of C_{max}/C_{in}. A possible explanation for this to occur more relevantly with nano- than with microiron slurries relies on the stronger magnetic interactions between particles in the former dispersion (*7*). Despite the stabilization introduced by the presence of xanthan gum in the dispersion, the formation of large aggregates, subject to filtering or ripening in the porous medium, cannot be totally ruled out (*11, 28*). Table 1 displays the overall iron particle yield (η), expressed as the ratio of the total eluted (M_{out}) and injected (M_{in}) iron mass during the whole length of each experiment (t), calculated through following expression (eq 1):

$$\eta = \frac{M_{out}}{M_{in}} = \frac{\int_0^t C_{out}\mathrm{d}t}{C_{in}t_{in}} = 1 - \frac{M_r}{M_{in}} = 1 - \frac{An\int_0^L C_r\mathrm{d}x}{M_{in}} \quad (1)$$

Where C_{in} and C_{out} are the iron concentration in the slurry phase at the inlet and at the outlet of the column, respectively; M_{in}, M_{out}, M_r are the mass of iron injected into the column, extracted at the outlet and resident, respectively; A is the area of the column section; n is the porosity; L the length of the column; t_{in} and t_{PV} are the duration of the whole iron injection phase and of the single PV injection, respectively.

The fraction of iron eluted by the end of the injection phase (η'), obtained by substituting t_{in} to t in eq 1, is also reported in table 1. In all experimental conditions, the nanoiron exhibits a lower η' value than the microiron, suggesting once again a deposition of the former particles within the column during the injection. Additionally, a linear relation was discerned between the mass of material still trapped in the column at the end of the injection phase (M_r) and the pressure drop between inlet and outlet at the same time (P_{max}), supporting the assumption that an increase in pressure during the injection is an indicator of column clogging (Figure 2). The high η values, exceeding 92% in all experiments (Table 1), however, seem to indicate that the latter phenomenon could be reversible. By flushing the column with water after injecting the slurry most of the material filtered in the previous phase seems to be removed, providing a very large iron recovery.

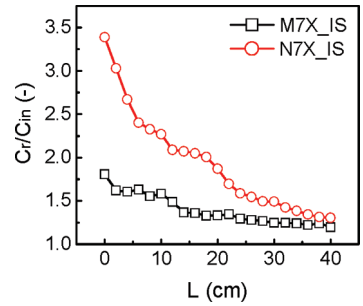

FIGURE 3. Distribution of ZVI (—○— NZVI, —□— MZVI) along the length of the column at the end of injection, expressed as if all the iron were present in the liquid phase and normalized to C_{in}.

Effect of the Ionic Strength and of Long-Lasting Injections on ZVI Transport. The transport of the two materials was also investigated under porewater chemistry relevant for field application. An IS of 12.5 mM (8 mM NaCl and 1.5 mM $CaCl_2$), a reasonable value for natural groundwater, was chosen to carry out the related tests. As for the DLVO theory, an increase in IS is expected to compress the electrical double layer of both particles and solid grains, leading to an increased particle aggregation and adsorption onto the solid matrix. However, the transport of both micro and nanoiron slurries in our experiments was hardly affected, the only effect being a slightly lower recovery of the microparticles (Table 1). This is due to the presence of the xanthan gum coating. Although the polymer is a negatively charged electrolyte and would be expected to be influenced by the IS, highly concentrated xanthan gum solutions have been shown to be relatively insensitive to salt concentration, consistently with our results (*21, 22*). A longlasting (26 PV) experiment was also conducted in order to preliminarily investigate the feasibility of a remediation intervention, which would require large volumes and long injections of reactive slurries, in order to reach the contamination target. The overall recovery of iron was comparable to the other experiments in the case of MZVI, and only slightly lower in the case of NZVI. In addition, despite the M26X and N26X experiments were almost 4 times as long as the other ones, the iron accumulated at the end of the injection phase was only slightly higher for the microparticles and approximately double for the nanoparticles in the long experiment as compared to the shorter experiments, as can be seen in Table 1. This suggests that the accumulation process is not linearly dependent on the total amount of material injected into the column and that the efficiency of xanthan gum as a delivery vehicle is not strongly affected by longer injection times, as is evident from the high recovery values reported in table 1 also for these experiments.

Distribution of ZVI along the Column. An additional measurement with a susceptibility sensor coaxial to the column was carried out at the end of the injection phase for experiments N7X_IS and M7X_IS. The susceptibility value along the length of the column was measured in static conditions before flushing the column with water. The values obtained provided information about the residual iron concentration (C_r) normalized to the total magnetic material (C_{in}) along the column length. A unitary distribution of C_r/C_{in} would be expected in the case of no aggregation and interaction with the solid matrix, whereas higher values would suggest particle deposition inside the porous media. The normalized concentration trends (Figure 3) are consistent with and support the findings obtained from the breakthrough curves and the pressure drop curves. The nanoscale iron appears to be trapped at the beginning of the column to a much higher extent than the microscale iron, whereas at the end of the column they have comparable concentrations. An almost uniform distribution of microscale iron

particle in similar conditions was also reported by Cantrell et al. (1997). The retained concentrations of iron measured by these authors is also consistent with our values of η.

Significance for Field Application. The exploitation of the magnetic properties of micro and nanoiron particles injected in the column to measure the breakthrough curve and the amount of material blocked along the length of the column proved extremely effective in our column experiments. This method allowed us to overcome the limitations—in terms of concentration of the slurry and of continuity of the measurement—that affect traditional breakthrough curve acquisition methods, i.e., spectrophotometric analysis of the elute (*9*−*12, 17, 20, 28, 29*). To our knowledge, this is the first column transport study using iron dispersions with concentrations as high as 20 g/L and able to provide continuous and reliable eluted concentration measurements, concentrations used in previous studies ranging from 0.1 to 6 g/L (*8*−*11, 16, 18, 27, 30, 31*). The efficiency of the magnetic susceptivimeter in our bench scale experiments and its being originally designed for geological and geophysical investigations on the field, suggest that measuring susceptivity to keep track of ZVI particles could be feasible also at a larger scale. In this sense, it could also be considered as a monitoring technique in field applications during groundwater remediation. Magnetic sensors could be installed in monitoring wells at increasing distances from the injection points to test the spatial distribution of the iron slurry.

As well as suggesting an innovative and valuable method for measuring indirectly ZVI concentration in suspension and present within sand packed columns, in this study we show evidence that the elution of 20 g/L ZVI suspensions through a porous medium can be greatly improved (to yields higher than 92%), if amended with xanthan gum and if injection of ZVI suspensions is alternated to water flushing. It is noteworthy that we used fairly coarse sand (0.5−1 mm) to pack the column, so further investigations need to be performed with finer and heterogeneous matrixes.

The effectiveness of xanthan gum relies on its capability of enhancing suspension stability and hindering particle aggregation. The mechanism of stabilization is kinetic rather than thermodynamic in nature, meaning that not only it reduces interaction potentials or avoids their expression—as in the case of electrosteric stabilization—but it also reduces motion of the particles by trapping them within the network of polymer chains, thus preventing aggregation. Moreover, the high viscosity of the polymer solution opposes higher drag forces to the particles motion, which would otherwise lead to aggregation and sedimentation (*21*). The shear thinning behavior of xanthan allows particles to remain suspended as a consequence of the high viscosity in the center of the pore space (where shear rates are low). Furthermore, the dispersion can easily flow in porous media since viscosity is low near the pore walls where high shear rates are experienced (*16, 21, 32*). These properties also guaranty a homogeneous permeation of the porous media regardless of permeability heterogeneities thanks to the absence of viscous fingering (*33*−*35*).

In terms of field application, obtaining such a high yield is extremely promising, since successful transport of highly concentrated iron dispersions is an essential prerequisite for real scale remediation interventions on site. In order to minimize the volumes of material injected in the subsurface, the concentration of required reactive material to address the contamination can rise very easily and is likely to be of the order of several 10s of g/L (*36*). Highly concentrated slurries are preferable mainly due to the risk of contaminant displacement and iron passivation which may occur if large volumes of dilute suspensions are employed (*37*). Additionally, higher solid loadings are likely to reduce transport costs from the synthesis facility to the contaminated site (*21*). It should be noted, however, that the results here reported refer to a one-dimensional geometry. As such, they provide preliminary understanding of the possibilities of enhancing ZVI micro- and nanoparticles transport by xanthan gum amendment. Further tests, both at laboratory and at pilot scale, need to be performed to assess these possibilities in a more complex setting, in particular in three-dimensional geometries, in order to mimic more closely real aquifer conditions.

Acknowledgments

The authors want to acknowledge Silvia Comba for her helpful suggestions during lab tests.

Literature Cited

(1) Zhang, W. X. Nanoscale iron particles for environmental remediation: An overview. *J. Nanopart. Res.* **2003**, *5* (3−4), 323–332.
(2) Tratnyek, P. G.; Johnson, R. L. Nanotechnologies for environmental cleanup. *Nano Today* **2006**, *1* (2), 44–48.
(3) Di Molfetta, A.; Sethi, R. Clamshell excavation of a permeable reactive barrier. *Environm. Geol.* **2006**, *50* (3), 361–369.
(4) Gillham, R. W.; Ohannesin, S. F. Enhanced degradation of halogenated aliphatics by zero-valent iron. *Ground Water* **1994**, *32* (6), 958–967.
(5) Elimelech, M.; Gregory, J.; Jia, X.; Williams, R. A., *Particle Deposition and Aggregation*; Butterworth-Heinemann: Woburn, MA, 1995.
(6) Phenrat, T.; Saleh, N.; Sirk, K.; Tilton, R. D.; Lowry, G. V. Aggregation and sedimentation of aqueous nanoscale zerovalent iron dispersions. *Environ. Sci. Technol.* **2007**, *41* (1), 284–290.
(7) Dalla Vecchia, E.; Coisson, M.; Appino, C.; Vinai, F.; Sethi, R. Magnetic characterization and interaction modeling of zerovalent iron nanoparticles for the remediation of contaminated aquifers. *J. Nanosci. Nanotechnol.* **2009**, *9* (5), 3210–3218.
(8) Phenrat, T.; Kim, H. J.; Fagerlund, F.; Illangasekare, T.; Tilton, R. D.; Lowry, G. V., Particle size distribution, concentration, and magnetic attraction affect transport of polymer-modified Fe0 nanoparticles in sand columns. *Environ. Sci. Technol.* **2009**, in Press.
(9) Schrick, B.; Hydutsky, B. W.; Blough, J. L.; Mallouk, T. E. Delivery vehicles for zerovalent metal nanoparticles in soil and groundwater. *Chem. Mater.* **2004**, *16* (11), 2187–2193.
(10) He, F.; Zhao, D. Y.; Liu, J. C.; Roberts, C. B. Stabilization of Fe-Pd nanoparticles with sodium carboxymethyl cellulose for enhanced transport and dechlorination of trichloroethylene in soil and groundwater. *Ind. Eng. Chem. Res.* **2007**, *46* (1), 29–34.
(11) Saleh, N.; Sirk, K.; Liu, Y. Q.; Phenrat, T.; Dufour, B.; Matyjaszewski, K.; Tilton, R. D.; Lowry, G. V. Surface modifications enhance nanoiron transport and NAPL targeting in saturated porous media. *Environ. Eng. Sci.* **2007**, *24* (1), 45–57.
(12) Tiraferri, A.; Sethi, R. Enhanced transport of zerovalent iron nanoparticles in saturated porous media by guar gum. *J. Nanopart. Res.* **2009**, *11* (3), 635–645.
(13) Tufenkji, N.; Elimelech, M. Correlation equation for predicting single-collector efficiency in physicochemical filtration in saturated porous media. *Environ. Sci. Technol.* **2004**, *38* (2), 529–536.
(14) Saleh, N.; Kim, H. J.; Phenrat, T.; Matyjaszewski, K.; Tilton, R. D.; Lowry, G. V. Ionic strength and composition affect the mobility of surface-modified Fe-0 nanoparticles in water-saturated sand columns. *Environ. Sci. Technol.* **2008**, *42* (9), 3349–3355.
(15) Tiraferri, A.; Chen, K. L.; Sethi, R.; Elimelech, M. Reduced aggregation and sedimentation of zero-valent iron nanoparticles in the presence of guar gum. *J. Colloid Interface Sci.* **2008**, *324* (1−2), 71–79.
(16) Cantrell, K. J.; Kaplan, D. I.; Gilmore, T. J. Injection of colloidal Fe^0 particles in sand with shear-thinning fluids. *J. Environ. Eng.* **1997**, *123* (8), 786–791.
(17) Hydutsky, B. W.; Mack, E. J.; Beckerman, B. B.; Skluzacek, J. M.; Mallouk, T. E. Optimization of nano- and microiron transport through sand columns using polyelectrolyte mixtures. *Environ. Sci. Technol.* **2007**, *41* (18), 6418–6424.
(18) Kanel, S. R.; Choi, H. Transport characteristics of surface-modified nanoscale zero-valent iron in porous media. *Water Sci. Technol.* **2007**, *55* (1−2), 157–162.
(19) Sun, Y. P.; Li, X. Q.; Zhang, W. X.; Wang, H. P. A method for the preparation of stable dispersion of zero-valent iron nanoparticles. *Colloids Surf., A* **2007**, *308* (1−3), 60–66.

(20) Yang, G. C. C.; Tu, H. C.; Hung, C. H. Stability of nanoiron slurries and their transport in the subsurface environment. *Sep. Purif. Technol.* **2007**, *58* (1), 166–172.
(21) Comba, S.; Sethi, R. Stabilization of highly concentrated suspensions of iron nanoparticles using shear-thinning gels of xanthan gum. *Water Res.* **2009**, *43* (15), 3717–3726.
(22) Rochefort, W. E.; Middleman, S. Rheology of xanthan gum - salt, temperature, and strain effects in oscillatory and steady shear experiments. *J. Rheol.* **1987**, *31* (4), 337–369.
(23) Rodd, A. B.; Dunstan, D. E.; Boger, D. V. Characterisation of xanthan gum solutions using dynamic light scattering and rheology. *Carbohydr. Polym.* **2000**, *42* (2), 159–174.
(24) Whitcomb, P. J.; Macosko, C. W. Rheology of xanthan gum. *J. Rheol.* **1978**, *22* (5), 425–425.
(25) Gonzalez, J. M.; Muller, A. J.; Torres, M. F.; Saez, A. E. The role of shear and elongation in the flow of solutions of semi-flexible polymers through porous media. *Rheol. Acta* **2005**, *44* (4), 396–405.
(26) Bregar, V. B.; Pavlin, M. Effective-susceptibility tensor for a composite with ferromagnetic inclusions: Enhancement of effective-media theory and alternative ferromagnetic approach. *J. Appl. Phys.* **2004**, *95* (11), 6289–6293.
(27) Kanel, S. R.; Goswami, R. R.; Clement, T. P.; Barnett, M. O.; Zhao, D. Two dimensional transport characteristics of surface stabilized zero-valent iron nanoparticles in porous media. *Environ. Sci. Technol.* **2008**, *42* (3), 896–900.
(28) Sirk, K. M.; Saleh, N. B.; Phenrat, T.; Kim, H. J.; Dufour, B.; Ok, J.; Golas, P. L.; Matyjaszewski, K.; Lowry, G. V.; Tilton, R. D. Effect of adsorbed polyelectrolytes on nanoscale zero valent iron particle attachment to soil surface models. *Environ. Sci. Technol.* **2009**, *43* (10), 3803–3808.
(29) Kanel, S. R.; Nepal, D.; Manning, B.; Choi, H. Transport of surface-modified iron nanoparticle in porous media and application to arsenic(III) remediation. *J. Nanopart. Res.* **2007**, *9* (5), 725–735.
(30) Reddy, K. R.; Karri, M. R. In *Electrokinetic Delivery of Nanoscale Iron Particles for In-Situ Remediation of Pentachlorophenol-Contaminated Soils Internationa Symposium on Geo-Environmental Engineering for Sustainable Development*; Han, B.; Hu, L., Eds.; Xuzhou: China, 2007.
(31) Zhan, J. J.; Zheng, T. H.; Piringer, G.; Day, C.; McPherson, G. L.; Lu, Y. F.; Papadopoulos, K.; John, V. T. Transport characteristics of nanoscale functional zerovalent iron/silica composites for in situ remediation of trichloroethylene. *Environ. Sci. Technol.* **2008**, *42* (23), 8871–8876.
(32) Oostrom, M.; Wietsma, T. W.; Covert, M. A.; Vermeul, V. R. Zero-valent iron emplacement in permeable porous media using polymer additions. *Ground Water Monit. Rem.* **2007**, *27* (1), 122–130.
(33) Homsy, G. M. Viscous Fingering in Porous-Media. *Annu. Rev. Fluid Mech.* **1987**, *19*, 271–311.
(34) Martel, R.; Hebert, A.; Lefebvre, R.; Gelinas, P.; Gabriel, U. Displacement and sweep efficiencies in a DNAPL recovery test using micellar and polymer solutions injected in a five-spot pattern. *J. Contam. Hydrol.* **2004**, *75* (1−2), 1–29.
(35) Zhong, L.; Oostrom, M.; Wietsma, T. W.; Covert, M. A. Enhanced remedial amendment delivery through fluid viscosity modifications: Experiments and numerical simulations. *J. Contam. Hydrol.* **2008**, *101* (1−4), 29–41.
(36) Varadhi, S. N.; Gill, H.; Apoldo, L. J.; Liao, K.; Blackman, R. A.; Wittman, W. K., Full-Scale Nanoiron Injection for Treatment of Groundwater Contaminated with Chlorinated Hydrocarbons. In *Natural Gas Technologies 2005 Conference*: Orlando, FL, 2005.
(37) Gavaskar, A.; Tatar, L.; Condit, W. *Cost and Performance Report Nanoscale Zero-Valent Iron Technologies for Source Remediation*; Naval Facilities Engineering Command: Port Hueneme, CA, 2005.

ES901897D